Preparation and In Vitro Thermo-Mechanical Characterization of Electrospun PLGA Nanofibers for Soft and Hard Tissue Replacement

*H. Fouad[1], T. Elsarnagawy[2], Fahad N. Almajhdi[3], and Khalil Abdelrazek Khalil[4, *]*

[1]Biomedical Engineering Dept., Faculty of Engineering, Helwan University, Egypt
[2] Faculty of Engineering, Prince Sultan University, Saudi Arabia
[3] College of Science, Dept. of Botany and Microbiology, King Saud University, Saudi Arabia
[4]Mechanical Engineering Dept., College of Engineering, King Saud University P.O. Box 800, Riyadh 11421, Saudi Arabia.
[*]E-mail: kabdelmawgoud@ksu.edu.sa

In this paper, aligned PLGA nanofibrous scaffolds were synthesized by electrospinning for tissue engineering. Morphological characterization showed highly aligned nanofibrous morphology with nearly uniform diameter less than 200 nm and porosity reaches to 73%. The FTIR results showed no changes in the FTIR spectra whether the material is in the bulk or nanofiber form. The thermo-mechanical properties were characterized by using thermogravimetry (TG) and differential scanning calorimetry (DSC). The results of thermal analysis confirmed that the amorphous nature of PLGA with glass transition temperature of the electrospun sheet is lower than that of the raw PLGA due to high surface area. The results of dynamic mechanical analysis (DMA) showed a strong dependence of the visco-elastic behavior of PLGA nanofibers in terms of the frequency and the temperature criteria as the storage modulus (G') increases at the time the loss modulus (G'') decreases with frequency. In vitro degradation behaviors of PLGA nanofibrous scaffolds were systematically investigated up to twenty weeks in phosphate buffer saline solution at 37°C. The visco-elastic behavior of PLGA nanofibrous scaffolds were evaluated during in-vitro degradation. As degradation time increases, the PLGA scaffolds show more weight loss and reduction in the storage modulus. The value of storage modulus was less than the half of its initial values after 12 weeks. In a ward, the aligned nanofibrous scaffolds used in this study constitute a promising material for tissue engineering.

1. INTRODUCTION

The tissue engineering is aimed at the recovery of the functionality of damaged tissues in-vivo and in vitro reconstruction of tissue architecture while realizing exquisite tissue-specific functions [1-

5]. In this strategy, a two and three-dimensional porous scaffolds with suitable degradation rate is necessary to accommodate the transplanted cells as a supportive matrix and to guide the formation of new tissue. Various scaffolds were prepared from natural and synthetic polymers for the soft and hard tissue replacement [6-12]. Naturally-derived scaffolds usually have hydrophilic surfaces and specific cell interaction peptides, which are excellent for cell growth. The weak mechanical properties and/or thermal stability of theses polymers limit their use in hard tissue replacement such as bone and cartilage repairs [5]. On the other hand, synthetic polymers can easily be formed into designed shapes with relatively high mechanical properties, but their hydrophobic surface is not favorable for cell seeding [5, 13]. The ideal scaffold for tissue replacement and repair should have good cell affinity and enough mechanical strength to serve as an initial support. Usually, biodegradable polymeric scaffolds can be fabricated by using particulate leaching [14], high-pressure gas expansion [15], gas formation [16], phase separation [17] and emulsion freeze-drying methods [18]. Furthermore, Porous scaffolds for tissue engineering should have high porosity as well as large interconnected pores with a view to allowing accommodation of large number of cells and facilitating uniform distribution of cells and diffusion of oxygen and nutrients [6-10]. To overcome these problems, a two dimensional nanofibrous mat is suggested.

Over the past few years, there has been increasing interest in ultrafine polymer fibers for biomedical applications, in particular in drug-impregnated. As the biodegradable ultrafine fibers are considered very effective for topical drug administration and wound healing because the ultrafine fibrous webs have unique properties such as high surface-to-volume ratios, small pore sizes, and high porosity. There are several techniques used for the production of polymeric ultrafine fibers, one of them is the electrospinning technique [8, 12, 19, 20]. This technique acquired more interest in recent years because of its versatility and potentiality for usage in different applications. This technique was popular due to its simple process operation, high performance in nanofiber fabrication, low-cost setup of required devices which consist of high voltage generator, syringe pump, and grounded collector. The procedure involves applying a very high voltage to syringe and pumping a polymer solution through it. The electrospun nanofibers of polymer are collected as a nonwoven fabric on a grounded plate below the syringe. Currently, several polymers have been successfully produced into ultrafine (nano /micro) fibers by electrospinning such as PVA, PEO, PLLA, PGA, PLGA, PCL silk, fibrinogen, collagen, gelatin, and chitosan. Due to its good biodegradability, biocompatibility and proper mechanical properties, Poly Lactic-co-Glycolic Acid (PLGA) is considered one of the most popular biodegradable polymers approved by the U.S. Food and Drug Administration [21]. PLGA has been widely investigated for its applicability in drug-delivery applications, surgical implants and tissue engineering scaffolds [19, 20]. Many studies have been concerned with the characterization of the biological behavior of 2D PLGA scaffolds for tissue replacement and drug delivery system [5, 12-15, 19-21]. On the other hand, few studies have been concerned with investigating the changes in the physical and thermal properties of electrospun PLGA nanofibers compared to the bulk material. These properties may be useful for predicting the degradation rate and selecting the suitable sterilization technique for the PLGA nanofibrous scaffolds.

The present study is a part of research project that is indented to fabricate and characterize 2D and 3D biodegradable PLGA scaffolds that is suitable for soft and hard tissue replacement using the

electrospinning technique. In this project, the effects of different spinning parameters (volt, viscosity, and spinning distance) on the electrospun nano fibers morphology, thermal, mechanical and biological properties will be studied. Also, the effects on the different scaffold properties due to heat treatment will be studied. Finally, the effects on the scaffolds degradation and cell growth due to different treatment will be investigated. The main objectives of this part of project are (1) fabricating of PLGA nanofibers scaffolds using the electrospinning technique, (2) studying the morphology of electrospun PLGA nanofibers, (3) monitoring the changes in the physical and thermal properties of PLGA nanofibers compared to the bulk material and finally (4) evaluating the changes in the visco-elastic behavior of PLGA nanofibrous scaffolds after and during in-vitro degradation.

2. MATERIALS AND METHODS

2.1. Materials

Poly (DL-lactide-co-glycolide) (PLGA) copolymer with L/G ratio 75:25, IV (dl/g) 0.59, weight-average molecular weight 70,000 and 1.25g/cm^3 density were purchased from NaBond Company, China. Tetrahydrofuran (THF), dimethylformamide (DMF) solvents and Phosphate buffer saline (PBS) pellets that used in the experiment were purchased from Sigma Aldrich. It is worth mentioning that no further purification was made for the whole chemicals which used directly in this experiment.

2.2. Electrospinning of PLGA Nanofibers

To prepare nanofibers by electrospinning, high voltage was applied to a polymer solution, where upon a charged jet is ejected from the needle and then undergone extensive stretching and thinning during a rapid solvent evaporation stage. While the jet travels towards the grounded collector, polymer fibers are formed (Figure 1). The electrospinning process is governed by a variety of forces including the Coulomb force between the charges on the jet surface, the electrostatic force of the external electric field, the viscoelastic force of the solution, the surface tension, the gravitational force, and the frictional force of air drag [21]. Nanofibers of polymer which was collected as a nonwoven fabric showed a number of unique characteristics such as large surface area-to-volume ratio and high porosity with very small pore size. These unique characteristics make the nanofibers excellent candidates for tissue engineering scaffolds. The PLGA nanofibers were prepared by electrospinning a PLGA solution (1–10 wt %) in DMF/THF (10-90 wt %). The nanofibers were collected on a target drum placed 30 cm from the syringe tip. A voltage of 20 kV was applied to the collecting target by a high voltage power supply, and the flow rate of the solution was 0.1 mL/h.
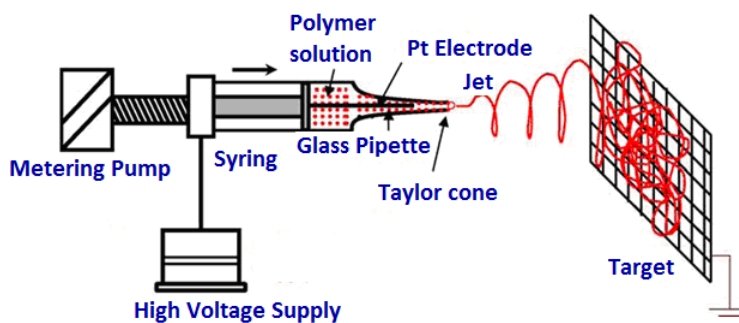
Figure 1. Schematic of the electrospinning apparatus

2.3. Characterization Methods

The morphological studies of PLGA Polymer and PLGA nanofibers were examined using Joel, USA, scanning electron microscope (JEOL GSM-6610LV) at an accelerated voltage of 5-10KV. Prior to SEM examination, specimens were coated with a thin layer of gold to dissipate the build-up of heat and electrical charges.

FT-IR was performed in the attenuated total reflection (ATR) mode by using a Bruker Spectrum Tensor 27 system equipped with an ATR cell with a diamond reflection element. This machine was used for measuring and scanning the IR transmittance spectra of bulk and PLGA nanofibers. Specimens were applied directly onto the surface of ATR crystal. Spectra resulted from the accumulation of 16 scans at 4 cm^{-1} resolution. The wavenumber range was 4000–400 cm^{-1}.

For determination of the electrospun nanofibers porosity, the nanofibers sheet apparent density was firstly estimated by the measurement of volume and mass of samples (8 samples at least) as the following equation. $Apparent density\ (g/cm^3) = \dfrac{Mass\ of\ nanofiber sheet\ (g)}{Volume of\ sheet\ (cm^3)}$

The porosity of scaffolds was then estimated, using the following equation.

$$Porosity\ (\%) = \left(1 - \frac{\rho}{\rho_o}\right) x\ 100\%$$

where ρ is the density of the electrospun sheet and ρ_o is the density of the bulk PLGA (1.25g/cm^3).

To determine the degradation rate of PLGA nanofibrous scaffolds, 10mm x 10mm specimens were sterilized by using ethanol and exposed to PBS solution. After weighting each specimen, the average initial weight M1 was calculated. Specimens were placed in incubator (36.6 °C, 5.5 % CO$_2$) to mimic the conditions which prevail during cell cultivation. The pH was monitored by phenol red color change. The medium was changed once a month when the pH did not decrease. At each time point (2, 4, 6, 10, 14, and 16 weeks), 4 specimens were removed from the buffer solution and weighed (M2) after drying in vacuum for 24 hours. The weight loss was measured as per the following equation:

$$\%\ weight loss = \frac{M_1 - M_2}{M_1}\ 100\%$$ where M1 and M2 are the weights of the nanofibers sheet before

and after degradation for t time, respectively.

Calorimetric measurements for bulk PLGA and PLGA nanofibers specimens were performed by means of Differential Scanning Calorimetry (Shimadzu -60). Each sample (5-10 mg) is sealed in an

aluminum pan and heated from 20 to 280 ^{o}C at rate of 5°C/min, then cooled down to 20°C at cooling rate of 5°C/min. The values of the transition temperature were obtained from the dynamic thermograms, using the midpoint between the intersections of the two parallel baselines, before and after the Tg. For calculating Tg from dynamic scans, at least three measurements was made for each sample to calculate the average value. The DSC results are used to investigate the changes in the thermal behavior of bulk PLGA material when fabricated in the nanofiber form by using the electrospinnig technique.

Thermogravimetric analysis (TGA) of the bulk and nanofiber of PLGA was conducted using a TA instrument (Q500 TGA, United States). The nanofibers sheets were kept under vacuum for 24 h prior to testing. The precisely weighed specimen was heated to 450°C at a rate of 10°C/min under nitrogen flow rate of 40 ml/min.

The viscoelastic behavior (storage and loss modulus) of PLGA nanofibers sheets was characterized by using a Dynamic Mechanical Analysis, DMA, via AR-G2 from TA, USA. The PLGA nanofibers sheets were tested over a frequency range from 0.1 to 600 rad/sec at temperature ranges 25°C. The DMA is also used to measure changes in the viscoelastic behavior of PLGA nanofibers due to changing the testing temperature.

3. RESULTS AND DISCUSSIONS

There are many important factors influencing the cell adhesion and proliferation such as surface properties, porosity and chemical composition which should be considered in the study of tissue engineering scaffold. The SEM micrographs (Figure 2) of the PLGA nanofibrous sheet showed a bead-free, highly aligned nanofibrous morphology with nearly uniform diameter less than micro scale range.
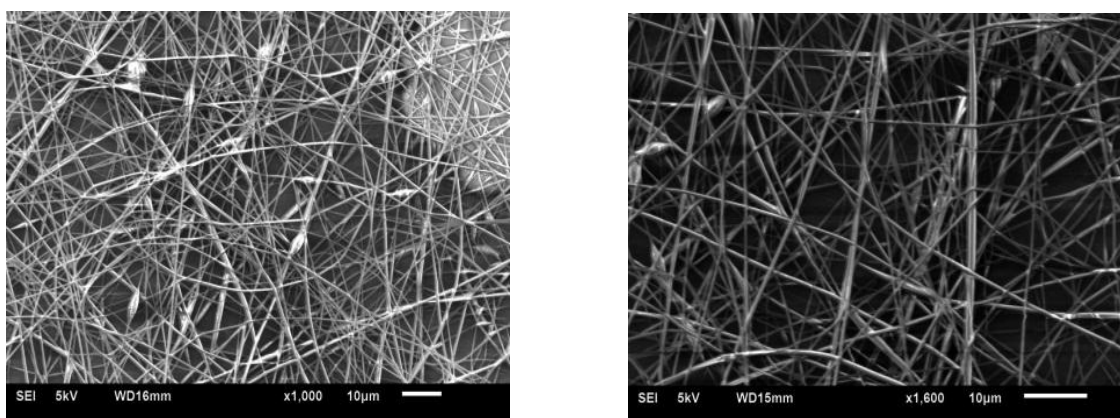

Figure 2. SEM micrographs of the electrospun PLGA meshes.
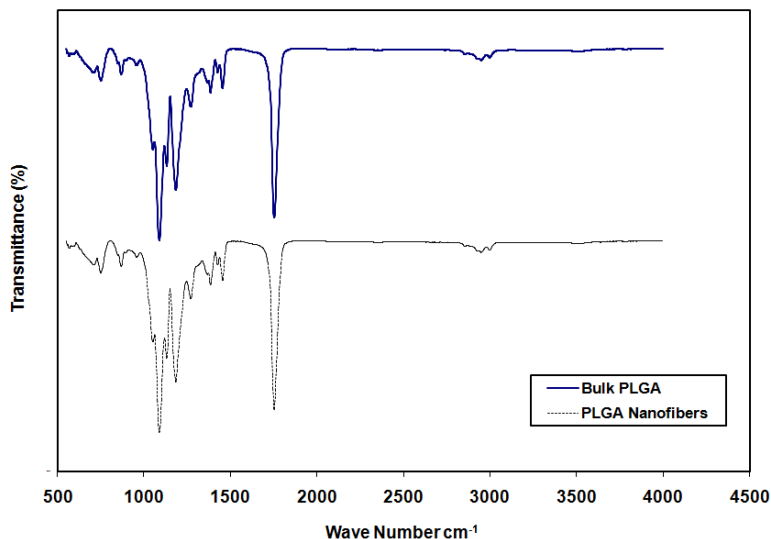
Figure 3. FT-IR spectrum of bulk and nanofibrous PLGA scaffold.

FTIR spectra for bulk PLGA and PLGA nanofibers are shown in Figure 3. Both spectra exhibit carbonyl stretching around 1,747 cm^{-1}, C-O bands in the 1,093–1,450 cm^{-1} regions in both spectra demonstrating the presence of the ester group. Bands around 3,000 cm^{-1} are present due to the alkyl groups. Similar peaks have been recorded for PLGA nanofibers by [23-24]. By comparing the spectra of bulk PLGA with PLGA nanofibers, it has been found that there are no changes in the FTIR spectra regardless of whether it is a bulk material or in the nanofiber form. Only the transmittance intensity of the PLGA nanofibers was increased may be as a result of the increase of unsaturated groups resulted from the cross-linking reactions.
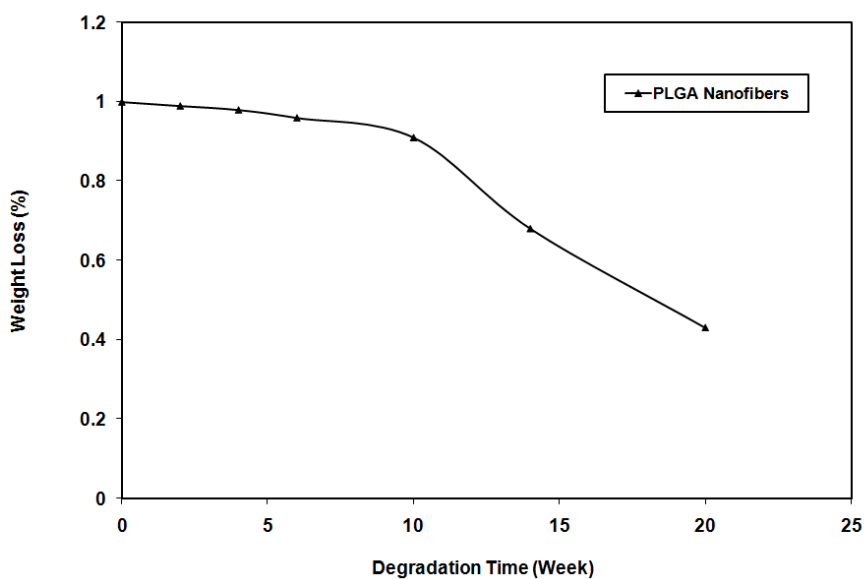

Figure 4. Degradation behavior of PLGA nanofibrous scaffolds in PBS at 37 $^{\circ}$C.

Porosity is considered an important parameter when selecting the nanofibrous scaffold for the cell culture experiment. The nanofibrous scaffolds can afford not only cell attachment, proliferation, and differentiation, but also sufficient transport for nutrients and waste removal. The apparent density and porosity of electrospun PLGA nanofibers sheet were calculated by using Equation (1) and (2). The calculated apparent density and porosity of PLGA nanofibers sheet fabricated with the electrospinning technique were found to be $0.465 g/cm^3$ and porosity of $73 \pm 3\%$ respectively. These highly porous scaffolds were beneficial for the adherence and proliferation of the cells. Similar values of PLGA nanofibers porosity (64% -71%) have been obtained by [25] when using the electrospinning technique for nanofibers fabrication.Figure 4 displays the weight loss of the degrading PLGA (75/25) nanofibrous scaffold as a function of the incubation time in the biological fluid. It can be seen that the loss in weight of the scaffold increases with the increase of degradation time. Initially, there is a gradual and slight reduction of the specimen weight that continues for several weeks. After 10 weeks, a dramatic decrease in mass is observed in agreement with previous studies on other PLGA based nanofibrous scaffolds [23, 26-27]. It was considered that the loss in weight of the scaffold can be attributed to the dissolved degradation products of the PLGA component.
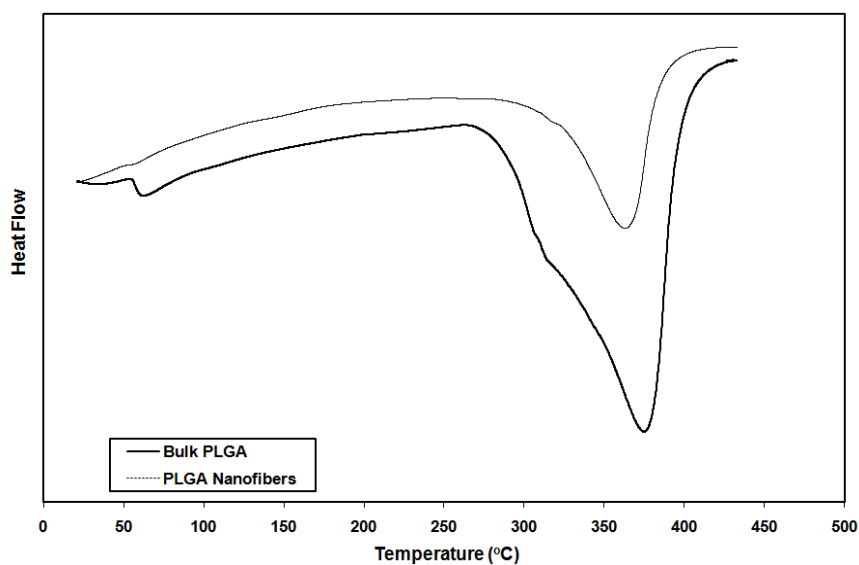

Figure 5. DSC Thermogram of neat as well as nanofibrous scaffold of PLGA

The thermal properties of bulk and electrospun PLGA nanofibrous sheets were examined by using DSC (Figure 5). The DSC thermogram confirms the amorphous nature of PLGA as it only shows the glass transition temperature (Tg) around 55°C and 51 °C for bulk PLGA and PLGA nanofibers respectively. The Tg of the electrospun sheet is lower than that of the raw PLGA. This could be due to the improvement in the orientation of molecular chains in the electrospun polymer nanofibers as well as the larger area to volume ratio of electrospun fibers. In addition, the crystallinity of the fiber structure is expected to decrease appreciably when compared to the raw PLGA materials. In other words, the chain entanglement in bulk form is much higher when compared to the same polymer in nanofiber form. Similar reduction in Tg of PLGA nanofibers compared to PLGA bulk material was

observed by other researchers [23-26]. The results indicated also that the decomposition temperature of PLGA nanofibers decreased from 371 ^{o}C to 360 ^{o}C when compared with bulk PLGA.

Figure 6 graphically displays the thermogravimetric analysis of bulk and PLGA nanofibrous sheet respectively. The weight loss vs. temperature profile of bulk and PLGA nanofibrous sheet shows that the weight of theses materials remain unchanged until the temperature of analysis reaches 240°C. These results show that the weight loss mainly occureds in the range of 260-380°C and 240-365 ^{o}C for bulk and PLGA nanofibrous sheet respectively with negligible change at temperature higher than 400°C. This weight loss indicates thermal decomposition or evaporation in the material. The present results indicated that the decomposition temperature of bulk PLGA material is higher than that of the nanofibrous PLGA sheet. This can be attributed to the possibility of the presence of residual solvents in the nanofiber sheet.
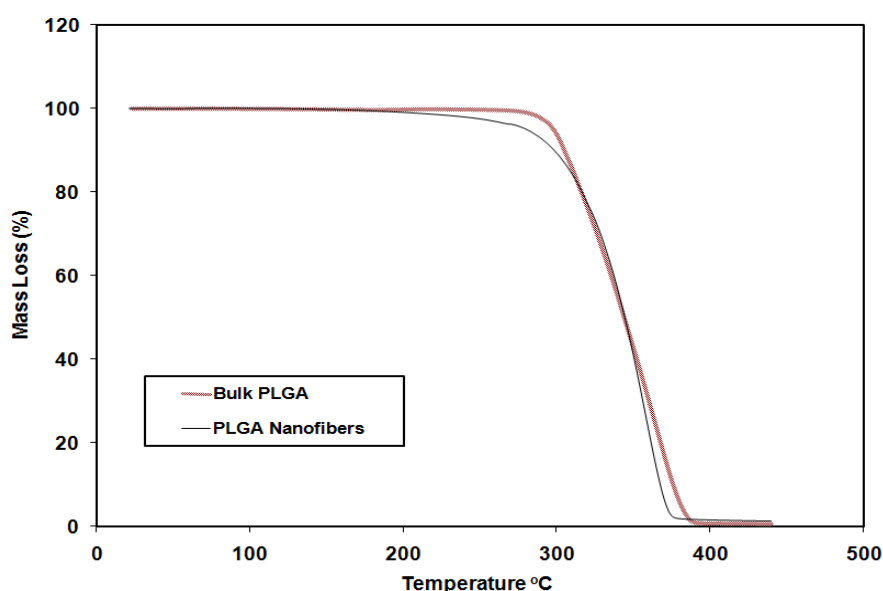

Figure 6. Thermogravimetric analysis (TGA) curves of bulk and nanofibrous PLGA scaffold

The response of storage and loss modulus (G', G") for PLGA nanofiber to the testing frequency is shown in Figure 7. The inset of Figure 7 shows G' and G" for a wider range of frequency. These results were realized at frequencies from 0.01 to 500 rad/sec at room temperature. The results show a strong dependence of the visco-elastic behavior of PLGA nanofibers on the test frequency (loading rate) and as expected the storage modulus, G', increases while loss modulus, G", decreases with frequency. These results confirm that the visco-elastic behavior of nanofibers is strain rate dependent. It is noticed that G' is more than G" and this assures that the elastic behavior of the material is dominant over the viscous one. As can be seen from Figure 7, the storage modulus increased from 150MPa to 230MPa when the testing frequency increased from 0.01 to 400 rad/sec.
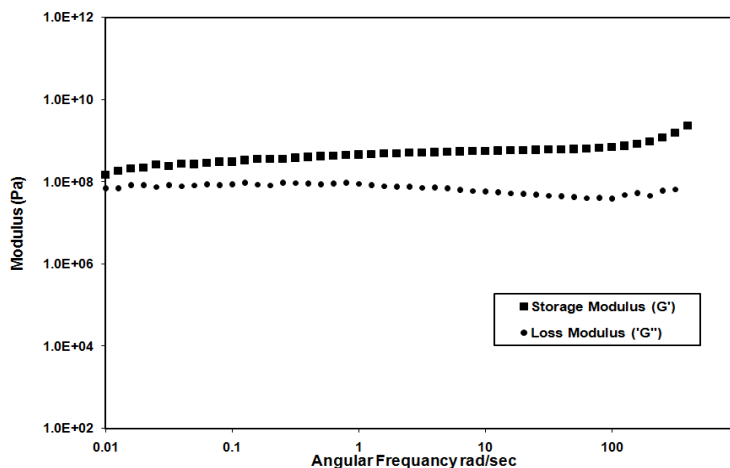
Figure 7. Variation of G' and G" with frequency for PLGA nanofibrous scaffold at room temperature
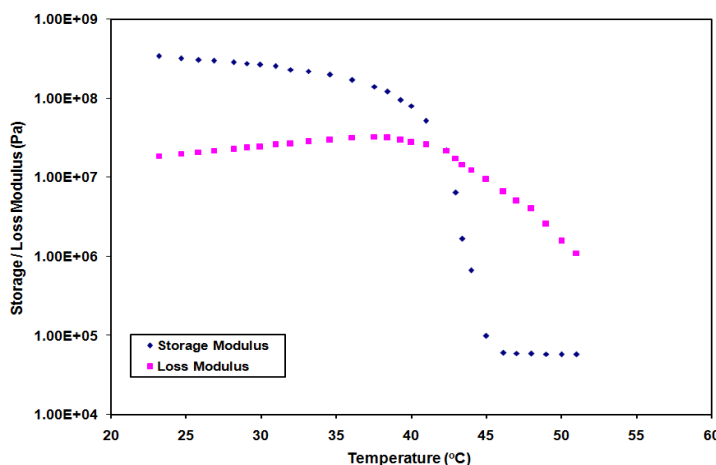

Figure 8. Variation of G' and G" with temperature for PLGA nanofibrous scaffold at 1rad/sec.

The temperature dependence of the storage modulus G' and G" for PLGA nanofiber is shown in Figure 8. For PLGA nanofibers, the storage modulus G' falls off around 43°C due to the glass transition that is clearly visible in the drop of G' and G". Because PLGA is amorphous polymer, no other peaks appear in the DMA curves. It is notable that the Tg values obtained through DMA and DSC are not exactly the same. This phenomenon has been discussed by other authors [28, 29]. These discrepancies are mainly attributed to the different operating principles of DMA and DSC as DSC is considered an instrumental thermal analytical technique while DMA is considered a dynamic mechanical technique. In addition, even for a specific method (DMA or DSC), the heating rate and loading frequency of the experiment can also influence the Tg value.

Figure 9 illustrates the change in storage and loss modulus of PLGA nanofiber scaffold with in-vitro degradation time. The storage and loss modulus of nanofibers was decreased with increasing the degradation time. After four weeks of degradation, the storage and loss modulus of nanofibers were decreased from 461 MPa and 92 MPa to 275MPa and 25MPa respectively at 1Hz. After 20 weeks of

degradation time, the storage and loss modulus were reduced to 65MPa and 6MPa respectively. However, the regenerated tissue in the nanofiber scaffolds can help to supporting these mechanical properties with degradation time. The reduction in the properties of PLGA nanofibers can be attributed to the polymer chain scission and the corresponding reduction in the molecular weight. However, as the degradation time increases, chain scission increases, resulting in a drop in the modulus values. Previous results [24] indicated that the elastic modulus of PLGA nanofibers and PLGA/HA composite decreases as the degradation time increases.
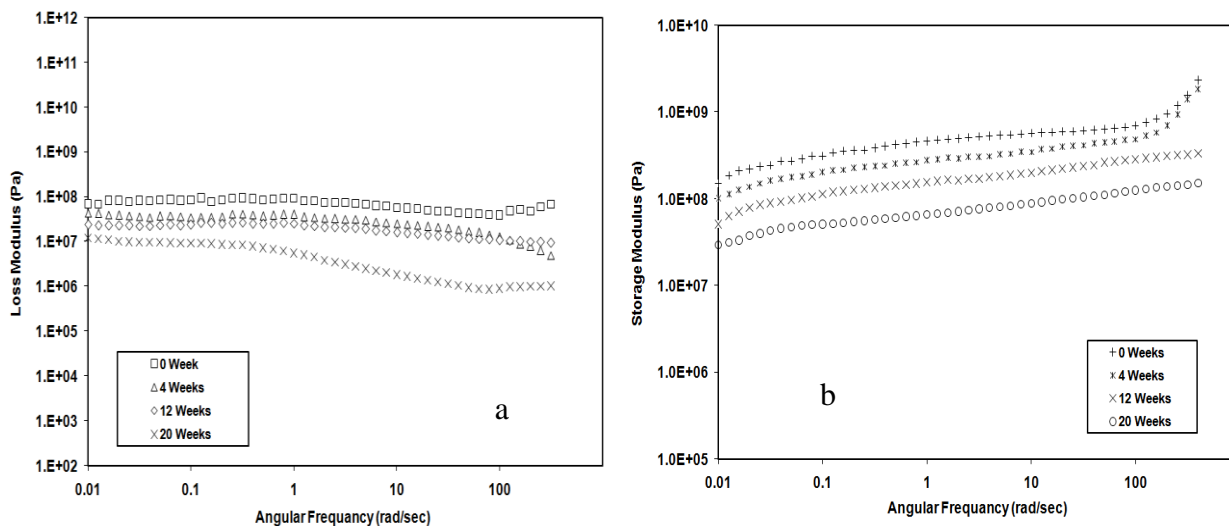

Figure 9. Variation of G' and G" with frequency and degradation time for PLGA nanofibrous scaffold at room temperature

4. CONCLUSIONS

In the present study, nanofibers of PLGA were prepared by electrospinning and ~~their~~ its properties including morphological, mechanical and thermo-mechanical properties, were investigated. The electrospun PLGA nanofibrous sheets showed highly aligned nanofibrous morphology with nearly uniform diameter less than micro scale range and porosity reaches to 73%. These good morphological properties can afford not only cell attachment, proliferation, and differentiation, but also sufficient transport for nutrients and waste removal. The FTIR results showed no changes in the FTIR spectra whether the material is in the bulk or nanofiber form. The thermal analysis results confirmed that the amorphous nature of PLGA with glass transition temperature of the electrospun sheet is lower than that of the raw PLGA due to the improvement in the orientation of molecular chains in the electrospun polymer nanofibers as well as the larger area to volume ratio of electrospun. TGA results show that the weight loss mainly occurs in the range of 240-380°C with negligible change at temperature higher than 400°C. The DMA results show a strong dependence of the visco-elastic behavior of PLGA nanofibers on the test frequency and temperature where storage modulus, G', increases while loss modulus, G", decreases with frequency. The results also showed that the storage modulus falls off around 43°C due

to the glass transition that is clearly visible. Also the DMA results showed that storage and loss modulus of nanofibers decreases significantly with increasing the degradation time in PBS.

References

1. J. Iwasa, L. Engebretsen , Y. Shima, M. Ochi, *Arthroscopy* 17 (2009) 561–577.
2. C. R. Lee, A. J Grodzinsky, H. P Hsu, M. Spector *Journal of Orthopaedic Research* 21 (2003) 272–281.
3. J. K. Sherwood, S. L. Riley, R. Palazzolo, S. C. Brown, D. C. Monkhouse, M. Coates, L. G. Griffith, L. K. Landeen, A. Ratcliffe. *Biomaterials* 23 (2002) 4739–4751.
4. U. Nöth , L. Rackwitz , A. Heymer, M. Weber , B. Baumann , A. Steinert , N. Schütze , F. Jakob , J. Eulert, *Journal of Biomedical Materials Research. Part A.* 83 (2007) 626–635.
5. W. Dai, N. Kawazoe, X. Lin , Dong J, Chen G. *Biomaterials* 31 (2010) 2141-2152
6. J. Glowacki, S. Mizuno, *Biopolymers* 89 (2008) 338–344.
7. F. Babaeijandaghi, I. Shabani, E. Seyedjafari, Z. S Naraghi, M. Vasei, V. Haddadi-Asl, K. K Hesari, M. Soleimani. *Tissue Engineering Part A* 16 (2010) 3527–3536.
8. S. K Tiwari, S. S Venkatraman. *Materials Science and Engineering: C* 32 (2012) 1037–1042
9. J. Yang, M. Yamato, T. Shimizu, H. Sekine, K. Ohashi, M. Kanzaki, T. Ohki, K. Nishida, T. Okano, *Biomaterials* 28 (2007) 5033-5043.
10. [L. Thorrez, J. Shansky, L. Wang, L. Fast, T. T. Vanden Driessche, M. Chuahc, D. Mooney, H. Vandenburgh, *Biomaterials* 29 (2008) 75–84.
11. A. Nieponice, L. Soletti, J. Guan, B. M. Deasy, J. Huard, W. R. Wagner, D. A. Vorp. *Biomaterials* 2008; 29: 825-833
12. A. Subramanian, U. M. Krishnan, S. Sethuraman, *Biomedical Materials* 6 (2011) doi:10.1088/1748-6041/6/2/025004
13. M. S. Kim, H. H. Ahn, Y. N. Shin, M. H. Cho, G. Khang, H. B. Lee. *Biomaterials* 28 (2007) 5137-5143.
14. A. G. Mikos, Thorsen AJ, Czerwonka LA, Bao Y, Langer R, Winslow DN, Vacanti JP. *Polymer* 35 (1994) 1068–1077
15. D. J Mooney, D. F Baldwin, N. P Suh, J. P Vacanti, R. Langer, *Biomaterials* 17 (1996) 1417–1422
16. Y. S Nam, J. J.Yoon, T. G.Park, *Journal of biomedical materials research* 53 (2000) 1–7
17. P. X Ma, R. Zhang, *Journal of biomedical materials research* 46 (1999) 60–72
18. K.Whang, C. H Thomas, K. E Healy, G. Nuber, *Polymer* 36 (1995) 837–842
19. T. Okuda, K. Tominaga., S. Kidoaki, *Journal of Controlled Release* 143 (2010) 258–264.
20. R. A Thakur, C. A Florek, J. Kohn, B. B Michniak. *International Journal of Pharmacology* 364 (2008) 87–93.
21. K. H Hong, S. H Woo, T. J Kang, *Journal of Applied Polymer Science* 124 (2012) 209–214
22. Y. Itoa, H. Hasuda, M. Kamitakahara, C. Ohtsuki, M. Tanihara, I. K. Kang, O. H. Kwon. *Journal of Bioscience and Bioengineering* 100 (2005) 43–49
23. I. Armentano, M. Dottori, D. Puglia, J. M. Kenny. *Journal of   Materials Science: Material in Medcine* 19 (2008) 2377–2387.
24. M. V Jose, V. Thomas, K. T Johnson, D. R Dean , E. Nyairo. *Acta Biomaterialia* 5 (2009) 305–315
25. F. Liu, R. Guo, M. Shen, S. Wang, X. Shi. *Macromolecular Materials and Engineering* 294 (2009) 666–672.
26. Y. J Liu, H. L Jiang, Y. Li, K. J Zhu. *Chinese Journal of Polymer Science* 26 (2008) 63-71.
27. L. Wu, J. Ding. *Biomaterials* 25 (2004) 5821–5830.

28. L. Wang, Z. Zhang, H. Chen, S. Zhang, C. Xiong, *Journal of Polymer Research* 17 (2010) 77–82.
29. O. J Yoon, C. Y Jung , I. Y Sohn , H. J Kim, B. Hong, M. S Jhon, N. E Lee. *Nanosheets. Composites: Part A* 42 (2011) 1978–1984.